Ultrasound in Medicine & Biology 000 (2026) 1–12

Contents lists available at ScienceDirect

Ultrasound in Medicine & Biology

journal homepage: www.elsevier.com/locate/ultrasmedbio

Original Contribution

Low-Frequency Ultrasound Enhances Osteogenic Differentiation Potential of Mesenchymal Stem Cells

Dhanak Gupta [a,*], Xuan Li [b,c], Jack Stevenson [b], Lisa Shriane [a], Hilde Metzger [b], Piero Miloro [d], Richard M Shelton [a], Ben A Scheven [a], Margaret Lucas [b], Anthony Damien Walmsley [a]

[a] School of Dentistry, University of Birmingham, Birmingham, UK
[b] Centre for Medical & Industrial Ultrasonics, James Watt School of Engineering, University of Glasgow, Glasgow, UK
[c] Department of Mechanical Engineering, Faculty of Engineering and Physical Sciences, University of Southampton, Southampton, UK
[d] National Physical Laboratory, Teddington, UK

ARTICLE INFO

Keywords:
In vitro ultrasound delivery
Mesenchymal stem cells
Bone regeneration
Peak negative pressure
Mineralisation
kHz frequency

ABSTRACT

Effects of ultrasound on mesenchymal stem cells (MSCs) have been investigated widely at MHz frequencies. However, the impact of kHz ultrasound frequencies on MSCs is unknown. This study investigated the effects of 25 kHz ultrasound on bone marrow-derived human MSCs. A 25 kHz transducer manufactured in-house was characterised and used to deliver ultrasound to MSCs in an *in vitro* experimental apparatus comprising of a degassed water-filled tank lined with ultrasound-absorbing tiles and an acoustically transparent non-traditional cell culture vessel called CLINIcell® cassette. Ultrasound field scans inside the tank confirmed absence of standing waves and peak negative pressure (PNP) ranges of 0, 0–45, 0–108 and 0–185 kPa with highest PNP at the centre of the cassette. Cells seeded in the cassette were exposed to continuous 25 kHz ultrasound for 5 min and immediately after treatment, cell death increased and metabolic activity decreased with increasing PNP, with most cell detachment at the centre of the cassette. Necrosis or apoptosis, accompanied by altered mitochondrial homeostasis (visualised via PINK1 and IP_3R immunocytochemistry), was found to be the mechanism of cell death. Two and five days post-treatment, a PNP of less than 108 kPa upregulated early osteogenic genes (*OSX, RUNX2* and *bGLAP*). Fourteen days post-treatment, a PNP of less than 45 kPa enhanced collagen production and mineralisation by 10% (measured via Sirius Red and Alizarin S Red staining). These findings suggest that a low ultrasound PNP (<45 kPa) at 25 kHz may offer potential therapeutic benefits applicable for bone regeneration.

Introduction

Mesenchymal stem cells (MSCs) residing within the bone marrow are critical for bone regeneration throughout the lifespan of skeletal hard tissue [1]. The routine application of ultrasound-based devices in medical procedures, such as bone healing [2] and osteotomy [3], has necessitated a clearer understanding of the interactions between MSCs and ultrasound energy.

High-power low-frequency ultrasound has applications in surgery, for example, in hard and soft tissue cutting and vessel sealing. Piezoelectric ultrasonic surgical devices, operating in resonance at a frequency in the range 20–100 kHz, are used as an alternative to conventional instruments [4] in dental [5], craniofacial [6], orthopaedic [7] and neurological procedures [8,9]. Al-Namnam et al. [10] recently reported that an ultrasonic scalpel (35 kHz) resulted in a 32%–36% reduction in the width of the zone of cell death at the cutting site in cartilage when compared with a standard conventional scalpel. A further understanding of cellular responses to excitation in this frequency range of ultrasound may improve hard and soft tissue recovery post ultrasonic treatment.

Significant attention has been focused on the effects of high-frequency (MHz) ultrasound on MSCs [11], but the influence of low-frequency ultrasound (20–100 kHz) on the survival and osteogenic differentiation potential of MSCs remains unclear. Low-frequency ultrasound has a longer wavelength and a wider beam that scatters more easily, leading to anomalies such as standing waves or unpredictable energy levels, respectively [12]. This makes it difficult to control ultrasound dose and relate it to biological effects, especially in traditional cell culture vessels [11,13], which have been used for the majority of *in vitro* investigations. Thus, there is a requirement for standardising kHz ultrasound exposure for accurate assessment of effects on cells.

Attempts have been made to minimise standing wave generation by placing the cell culture vessel in front of the ultrasound transducer, while both are immersed in a tank filled with degassed water [14,15]. Another study improved this system by also adding an ultrasonic absorber behind the sonicated sample [16]. Savva et al. [17] modified this setup further by

* Corresponding author. School of Dentistry, University of Birmingham, Birmingham, UK.
E-mail address: d.gupta@bham.ac.uk (D. Gupta).

https://doi.org/10.1016/j.ultrasmedbio.2026.03.026
Received 12 September 2025; Revised 3 March 2026; Accepted 30 March 2026

Please cite this article as: D. Gupta et al., Low-Frequency Ultrasound Enhances Osteogenic Differentiation Potential of Mesenchymal Stem Cells, Ultrasound in Medicine & Biology (2026), https://doi.org/10.1016/j.ultrasmedbio.2026.03.026

developing a new cell culture vessel called a Biocell, which was acoustically transparent and could be fully immersed in the tank. This enabled delivery of LIPUS doses at 1 MHz and 45 kHz to murine osteogenic cells for proliferation assessments. However, the biocell was manufactured specifically for the study and is not commercially available.

Beekers et al. [18,19] reported commercially available CLINIcell® cassettes as suitable for studying microbubble oscillation behaviour and ultrasound-mediated drug delivery in endothelial cells. Therefore, this study combines the use of CLINIcell® cassettes with a water-filled glass tank, fully lined with an acoustic absorber, to achieve two aims: first, to establish a novel methodology that standardises the assessment of kHz ultrasound *in vitro*, and second, to determine the effects of 25 kHz ultrasound on MSC survival, proliferation and osteogenic differentiation.

Materials and methods

All materials were purchased from ThermoFisher Scientific, UK unless described otherwise. All calorimetric assay measurements were undertaken using the Spark® multimode microplate reader. The design of the ultrasound transducer is explained in Supplementary data and illustrated in Figures S1 and S2.

In vitro *ultrasound exposure set up*

The ultrasound exposure system consisted of a tank (length 60 cm, height 30 cm and width 30 cm) lined with polyurethane acoustic absorber (50 mm thick, Apltile SF5048, Precision Acoustics, UK) on the base and vertical walls; the tank was then filled with deionised degassed water (Fig. S3). The 25 kHz transducer was fully immersed in the tank and driven by an ultrasonic driver (PDUS210 and TX3 Transformer, PiezoDrive). CLINIcell® cassettes (50 μm polycarbonate membranes, 25 cm^2 surface area, MABIO, Tourcoing, France), were chosen as the cell culture vessels [19–21] and were also immersed in the tank. The centre of each cassette was aligned with the centre-line of the transducer, with a separation distance of 5 mm from the transducer output face (Fig. 1).

The cells within the cassette were exposed to 25 kHz continuous ultrasound (with wavelength of 59.6 mm) for 5 min then either incubated further at 37°C, 5% CO_2 for 2 or 5 days or removed for assessment or reseeding. Four transducer driving current settings were selected, of 0 (control – no exposure), 0.01, 0.025 and 0.045 A, the latter three correlating with a low, medium and high ultrasound PNP. The water in the tank was maintained at 37°C using an electric immersion water heater (Tianbi Ceramics Co, Ltd, China) throughout the exposure period.

Ultrasound field characterisation

To measure the ultrasound pressure field in the tank, an initial transducer current of 0.025 A (Fig. 2) was selected. The pressure field was then mapped using a calibrated 4 mm needle hydrophone (Precision Acoustics), connected to an oscilloscope (PicoScope 3000 series, Pico Technology, UK). Five cycles of the waveform were captured in a sample window of 200 μs while the transducer was in steady-state operation. Three transverse area scans (10.5 cm × 8.5 cm) and one longitudinal area scan (8.5 cm × 2.5 cm) with respect to the transducer face were performed. The first transverse scan was recorded at 5 mm from the transducer face and the second at 25 mm; the third was again at 25 mm but with a deionised degassed water-filled cassette placed 5 mm from the transducer face. The longitudinal scan was started at 5 mm from the transducer face and moved along the length of the tank. The pressure field was measured for each of the transducer driving currents.

Human mesenchymal stem cell culture

Immortalised (Human mesenchymal stem cell) hMSCs were purchased (T0529, Applied Biological Materials Inc., Richmond, Canada). Cells were regularly passaged at a ratio of 1:3 when 80%–90% confluent. Until passage 5, the cells were cultured using PriCoat™ T25 Flasks (G299, ABM) and PriGrow III (TM003, ABM) with 10% (v/v) foetal bovine serum (FBS, 10270-106, Gibco™), 1% (v/v) penicillin/streptomycin (P/S) (Sigma, UK) at 37°C, 5% CO_2. At passage 6, the cells were transferred to Thermo Scientific™ Nunc™ cell-culture treated polystyrene and grown in 44.5% (v/v) PriGrow III, 44.5% (v/v) Dulbecco's Modified Eagle Medium (DMEM, 31885-023, Gibco™) with 10% (v/v) FBS and 1% (v/v) P/S. At passage 7 and beyond, the cells were transferred to 89.5% (v/v) DMEM with 10% (v/v) FBS and 0.5% (v/v) P/S, henceforth termed the standard culture medium (SC) [22].

Cells between passages 11 and 40 were used for experimentation. As different culture conditions may alter MSCs characteristics [23], the cells were analysed for hMSC characteristics including CD marker expression, specifically CD73 (APC-conjugated), CD105 (PerCP-conjugated) and CD44 (PE-conjugated) (all from BD Biosciences) using flow cytometry, and for multipotency (osteogenesis and adipogenesis), which were described for this cell line in its original state by the manufacturer. For osteogenic (OS) differentiation, SC was supplemented with 100 nM dexamethasone, 50 µg/mL ascorbic acid 2-phosphate and 0.5 mM beta-glycerophosphate [22]. For adipogenic (AD) differentiation, SC was supplemented with 100 nM dexamethasone, 100 µg/mL insulin, 0.2 mM indomethacin, 0.45 mM

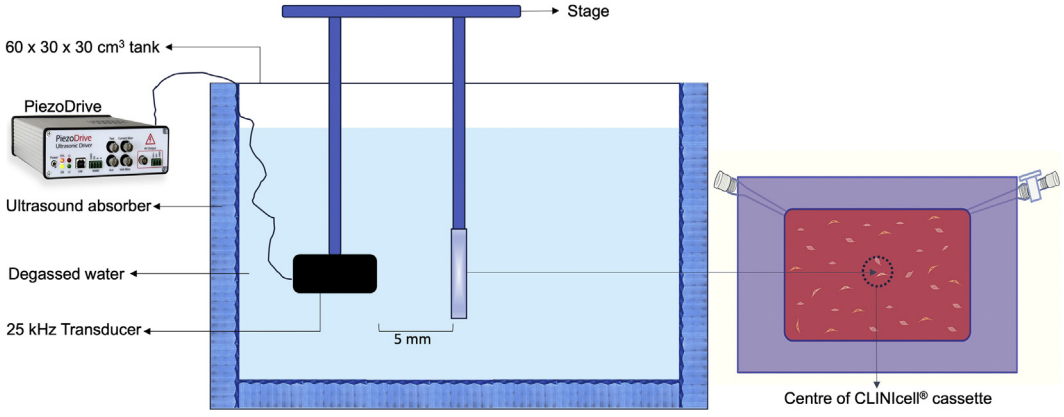

Figure 1. Diagram of *in vitro* ultrasound exposure set-up showing a side view of the degassed water-filled tank lined with ultrasound-absorbing tiles. The centre of the transducer front face and the centre of the CLINIcell® cassette were aligned at a distance of 5 mm from each other and 11 cm above the absorber surface for the delivery of ultrasound to the cells.

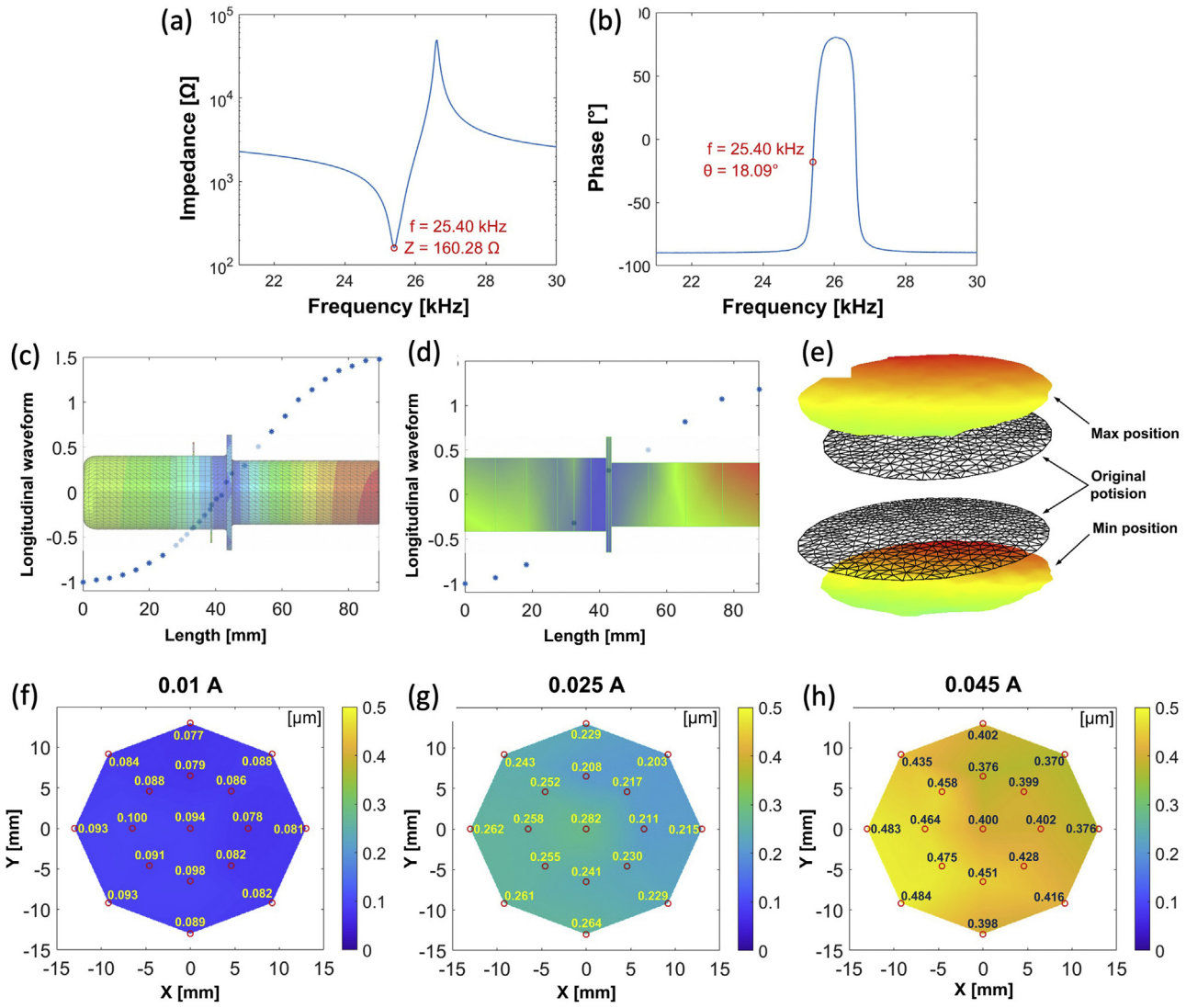

Figure 2. Transducer characterisation in air at low power including low power impedance spectroscopy showing (a) the 1st longitudinal mode impedance magnitude and (b) the impedance phase. Transducer dynamics were characterised by (c) an FEA model of the transducer showing the calculated longitudinal mode (warm to cool colours depict antinodal to nodal locations) with the longitudinal waveform also shown, and (d) EMA of the transducer using laser vibrometry, showing good agreement. The out-of-plane motion of the anterior face was measured (e) showing the displacement at the maximum and minimum of one vibration cycle of the transducer longitudinal mode, measured from a grid of measurement locations using a scanning 3D laser Doppler vibrometer. Notice the nonuniformity across the face (seen as red to green and also visible in the FEA model). The anterior face vibration displacement amplitudes (f–h) were characterised for currents of 0.01, 0.025 and 0.045 A, showing displacement increasing with current. EMA, experimental modal analysis; FEA, finite element analysis.

3-isobutyl-1-methylxanthine, 1 μM Roziglitazone [24]. The medium was changed every 2–3 days until day 21 of differentiation. Methodology for metabolic activity assay, real-time PCR, immunocytochemistry, DNA content assay, Alizarin Red S, Sirius Red and Oil O Red stainings are described in Supplementary data.

To investigate the immediate effects of ultrasound, cells were seeded at a density of 10,000 cells/cm^2 in CLINIcell® cassettes. The following day, cells within the cassettes were exposed to ultrasound in the tank and immediately assessed for morphology and detachment via actin/DAPI staining (Section 'Measurement of cell morphology and zone of cell detachment on CLINIcell® cassette') and for cell death via trypan blue staining. The markers of cell death were investigated using an apoptosis/necrosis assay via flow cytometry (Section 'Apoptosis/Necrosis assay'). To assess the effect of ultrasound on early osteogenic markers, expression levels for *OSX, RUNX2* and *bGLAP* (osteocalcin) genes (Table S1) using real-time PCR were assessed after 2 and 5 days of culture in cassettes post ultrasound exposure. For induction of osteogenic differentiation or immunocytochemistry after 24 h, the cells previously exposed to ultrasound were trypsinised to remove from cassettes and reseeded at 10,000 viable cells/cm^2 on well plates or Ibidi slides, respectively. The reseeded cells were also assessed for mitochondrial homeostasis via immunochemistry for PINK1 (phosphatase and tensin homolog-induced kinase 1, involved in mitophagy for removal of damaged mitochondria) and IP_3R (inositol 1,4,5-trisphosphate receptor, an intracellular calcium channel on the endoplasmic reticulum membrane known to respond to ultrasound [16]) after 24 h.

Measurement of cell morphology and zone of cell detachment on CLINIcell® cassette

Cells were washed with Dulbecco's phosphate buffer saline (DPBS) and fixed with 3.7% paraformaldehyde (Alfa Aesar) in phosphate-buffered saline (PBS) for 10 min at room temperature (RT). After a washing with DPBS and permeabilisation with 0.5% Triton

X-100 in DPBS, the cells were again washed with DPBS and stained with AlexaFluor™ 488 phalloidin (R37110) for 30 min at RT and then 1 μg/mL 4′,6-diamidino-2-phenylindole (DAPI) in DPBS for 5 min at RT [25]. Images were captured using a Nikon D5100 camera from an inverted Nikon ECLIPSE TE300 fluorescent microscope. To measure the zone of cell detachment after ultrasound treatment, multiple sequential images were taken across the breadth of the cassette film in the middle of the cassette (Fig. S4). The area occupied by actin-stained cells per image was measured using Image J software (version: 2.0.0-rc-69/1.52p).

Apoptosis/Necrosis assay

A GFP-CERTIFIED® apoptosis/necrosis detection kit (Enzo Life Sciences, Devon, UK) was used to assess cell death. The cells floating in culture medium and those attached on the cassette film were collected and stained according to the manufacturer's instructions. Samples were analysed using a CytoFLEX Flow Cytometer (Beckman Coulter Life Sciences) and CytExpert software (Beckman Coulter Life Sciences). For 7-aminoactinomycin D (7-AAD) only and annexin V only controls, cells were cultured with 1% saponin and 30% H_2O_2 solutions, respectively (Fig. S5).

Statistical analysis

Statistical analysis was performed using GraphPad Prism 10, version 10.1.0. (San Diego, CA, USA). All experiments were repeated twice with three wells or samples per condition per experiment. Simple linear regression was performed to compare trends of cell detachment in controls with cells exposed to 108 kPa ultrasound PNP in the cassettes. One-way analysis of variance was performed for cell counts, metabolic activity, protein expression, DNA content and cell differentiation assessments. p values < 0.05 were considered to indicate significant differences.

Results

Transducer characteristics

Impedance analysis identified the resonance frequency of the 1st longitudinal mode of the transducer as 25.4 kHz (Fig. 2a), with impedance magnitude and phase at resonance of 160 Ω and 18°, respectively (Fig. 2b). The 1st longitudinal mode predicted by finite element analysis (FEA) and measured by experimental modal analysis (EMA), using a laser Doppler vibrometer (LDV) are shown in Figure 2c,d, showing good agreement, with the mode shape nodal plane located at the transducer flange. Slight displacement nonuniformity is observed across the anterior face of the transducer (visible in Figure 2e–h).

LDV measurements from a grid of measurement points on the anterior face, when the transducer was vibrating in air under free conditions (Fig. 2f–h), show the increase in displacement amplitude as current was increased. The centre point of the transducer exhibited displacement amplitudes of 0.094, 0.282 and 0.400 μm and a mean ± S.D. of 0.087 ± 0.007, 0.239 ± 0.023 and 0.425 ± 0.039 μm across the 17 points measured when the transducer current was 0.01, 0.025 and 0.045 A, respectively. This amounted to 274% and 486% increase in the displacement amplitude of the transducer in air when the current increased from 0.01 to 0.025 A and 0.01 to 0.045 A, respectively. Vibration non-uniformity is evident in Figure 2f–h, consistent with the mode shape observed in Figure 2e, particularly at higher current levels (0.025 A and 0.045 A). For instance, in Figure 2h, the top-right region of the transducer's anterior face exhibits 30% lower displacement amplitude than the bottom-left region.

Ultrasound characteristics

The transverse scans (Fig. 3a–c) illustrate that 5 mm from the transducer face, the highest PNP occurred at the centre, which reduced by approximately 70% at 2.5 cm radially outwards from the centre. There was almost three times lower PNP at 25 mm from the transducer face and approximately 50% reduction in PNP at 2.5 cm radially outwards from the centre. For both scans, the pressure field was not symmetrical, in fact when the cassette was introduced between the transducer face and the scanning distance (25 mm), there was a second 'hot spot' at around $x = 40$ mm (Fig. 3c). The longitudinal scan (Fig. 3d) confirmed that the highest PNP was nearest the transducer face; however, the pressure field was not symmetrical around 0 mm in the XZ plane.

PNP at increasing driving current was measured (Fig. 3e,f) at 5 mm from the transducer anterior face, where the cassette was subsequently positioned for ultrasound exposure in cell culture experiments. The PNP in water increased linearly with transducer current. Based on this relationship between measured PNP and transducer driving current at 5 mm distance from the transducer face (Fig. 3e), it was deduced that the cells experienced PNPs of 0, 0–45, 0–108 and 0–185 kPa in the cassette with highest PNP in the centre of the cassette, for transducer current settings of 0 (control – no ultrasound), 0.01, 0.025 and 0.045 A, respectively. Moreover, the presence of the cassette did not significantly affect ultrasound propagation in the tank as the transmission percentage of the cassette (80%) was within the needle hydrophone accuracy of 13% –20%.

Characterisation of the hMSC cell line

Figure S6 shows CD marker expression as well as the osteogenic and adipogenic differentiation potential of the adapted immortalised hMSCs. The cells (>90%) expressed CD73, CD44 and CD105. When grown in OS medium, the cells demonstrated >10-fold increase in the expression of all the investigated osteogenic markers, namely, *RUNX2, bGLAP (osteocalcin)* and *SPARC (osteonectin*) compared with cells maintained in SC medium on days 7 and 14 in culture ($p < 0.05$). By day 21, there was 300 times higher calcium deposited in the extracellular matrix (ECM) by cells in OS medium compared with cells in SC medium ($p < 0.05$).

Cells maintained in AD medium showed a consistent increase in expression of *PPARγ, AP2* and *ADIPOQ* and a decrease in *GLUT4* expression, from day 7 to day 21 of culture ($p < 0.05$), whilst there were no significant changes observed in cells in the SC medium. By day 21, there were three times more lipids stained in the case of cells in AD medium compared with in SC medium ($p < 0.05$). The osteogenic and adipogenic assays indicated that the hMSCs were able to differentiate along both lineages.

Effect of ultrasound on cell survival and attachment in cassettes

After ultrasound exposure, the cells (those floating in the culture medium as well as the cells attached to the film) were collected and assessed for cell viability (Fig. 4a). The trypan blue exclusion assay showed a drop in mean percentage of live cells with increasing PNP ($p < 0.05$), where an average of 17% of the total cells died after exposure to 0 –185 kPa PNPs. The mean percentage metabolic activity per cassette (an indirect measure of number of cells that remained attached to the cassettes) decreased with an increase in ultrasound PNP ($p < 0.05$), with 27% reduction for 185 kPa highest PNP (Fig. 4b).

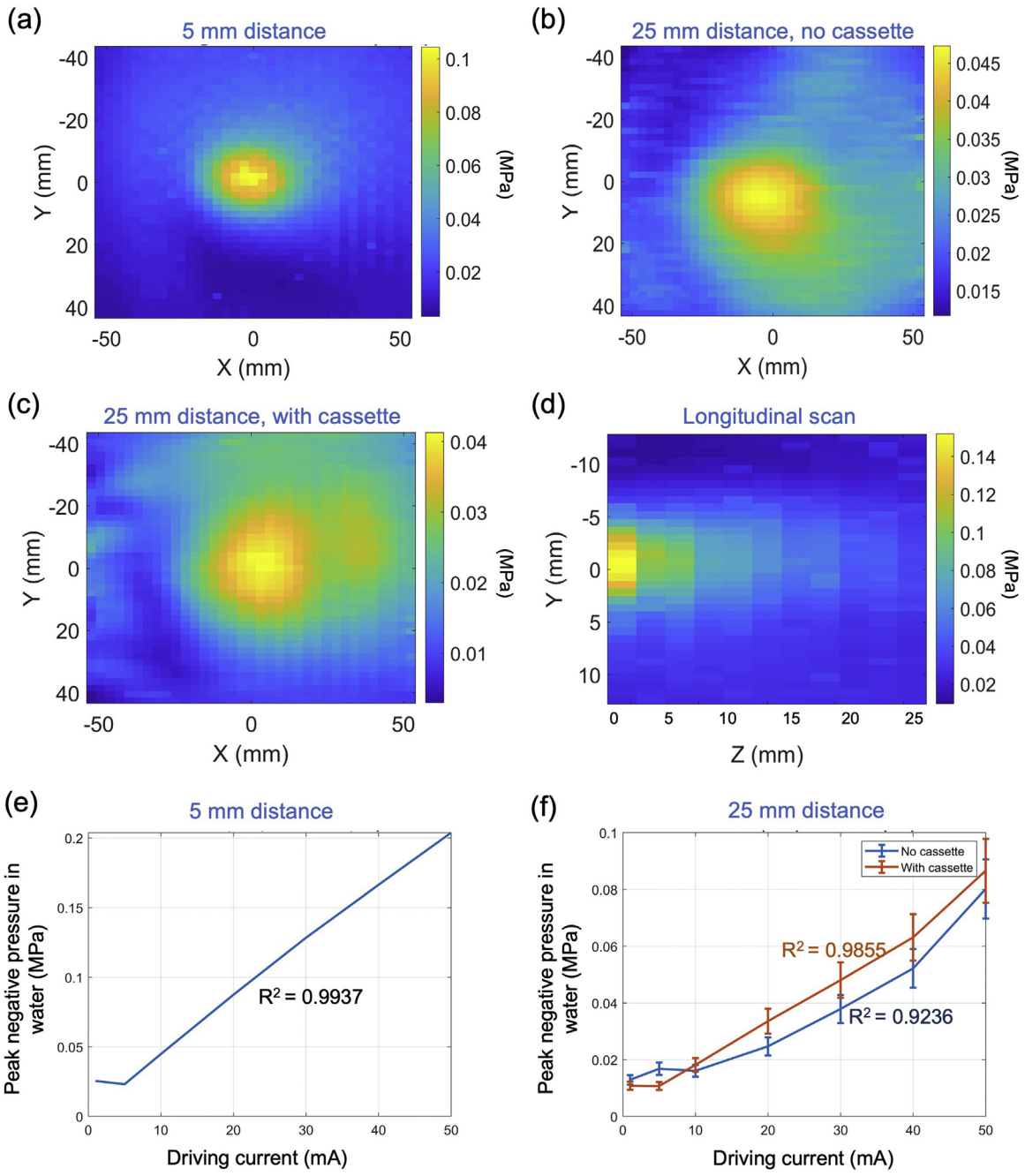

Figure 3. Characterisation of the ultrasound field in the tank. All transverse scans, at (a) 5 mm distance, (b) 25 mm distance without cassette and (c) 25 mm distance with cassette, showed a hotspot for PNP at the centre of the cassette. The longitudinal scan at 5 mm from the transducer along the length of the tank in (d) also showed a hotspot for PNP at the ultrasound source. The PNP increased as the transducer driving current increased from 0.005 to 0.04 A, at (e) 5 mm distance and (f) at 25 mm distance (with or without cassette in the wave path) away from the transducer. Error bars indicate a 13% measurement error. PNP, peak negative pressure.

Cell morphology was also assessed immediately after ultrasound treatment in cassettes (Fig. 4c). For the controls, the cells exhibited a characteristic spindle shape. Application of ultrasound caused some of the cells to round up and detach from the cassette film. The higher the PNP, the more cells detached from the centre of the cassette. As an example, the effect of 0–108 kPa ultrasound PNPs on an area covered by cells across the width of the cassette is shown in Figure 4d. On average, there was 42% reduction in area covered by the cells per image across the width of the cassette in the middle. Images from the central region of the cassette (where the ultrasound field is strongest) showed least cells or maximum cell damage, and this region was approximatively 1 mm wide. There were also two other regions away from the centre of the cassette ($p < 0.05$) on either side but the cell detachment here did not seem symmetrical in both directions, in line with the non-uniform nature of ultrasound field and the displacement measurements of the transducer face.

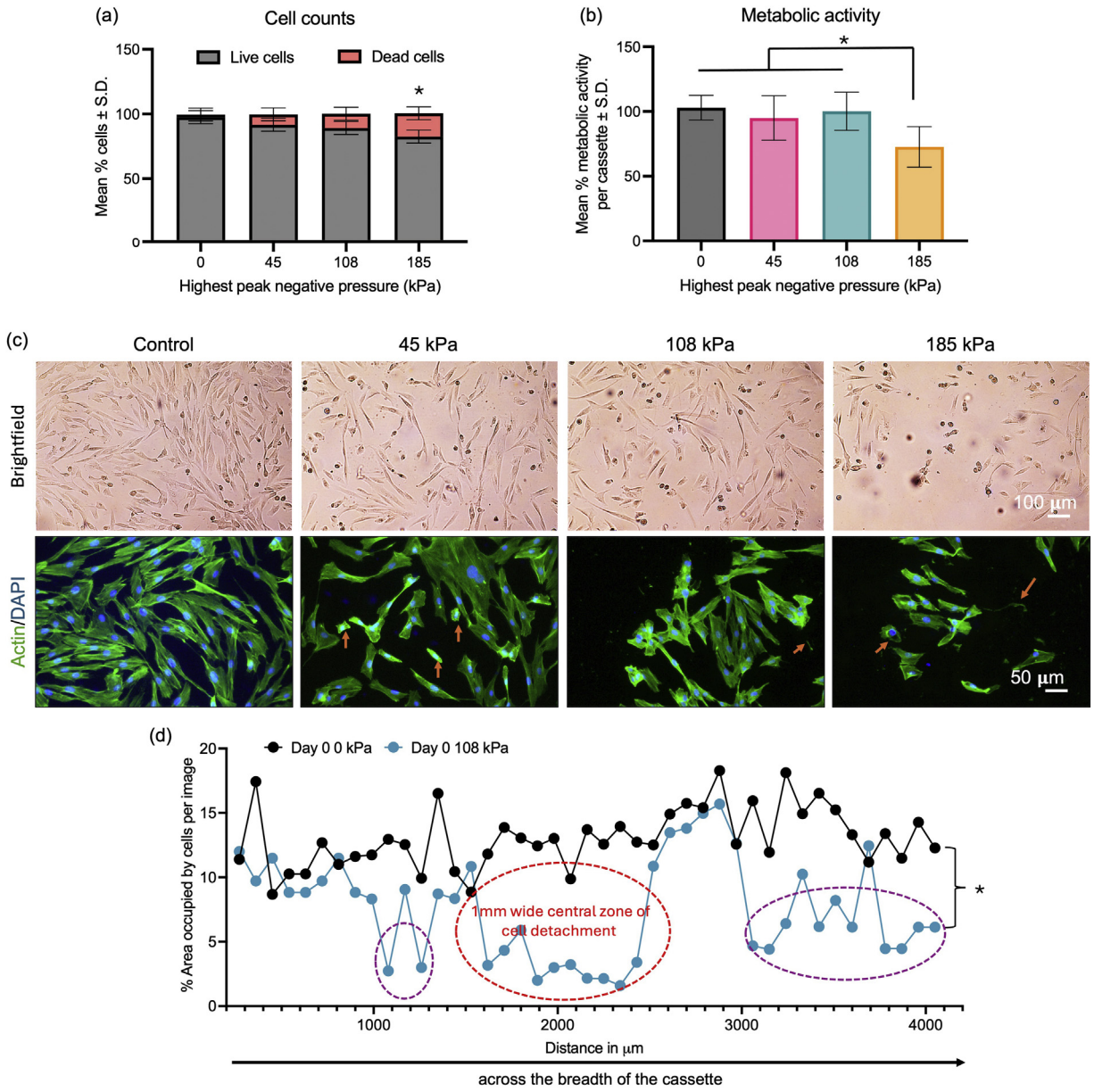

Figure 4. Assessment of immediate effects of ultrasound on cells on cassettes. There was increasing cell death due to increasing ultrasound pressure observed via (a) trypan blue exclusion assay (mean live or dead cell counts) and (b) metabolic activity assay. This trend was also visible through imaging with or without actin (*green*) and DAPI (*blue*) staining, shown in (c). The measurements for area occupied by cells per image across the width of the cassette with (0–108 kPa) or without ultrasound exposure in (d) showed a higher cell detachment in the centre of the cassette (aligned with the centre of the transducer) highlighted in the red dotted region. Other areas of cell death are highlighted in purple dotted region. * Indicates $p < 0.05$ relative to control, unless otherwise indicated, $n = 3$. DAPI, 4′,6-diamidino-2-phenylindole.

Mechanism of cell death after ultrasound treatment

A consistent increase in early apoptotic, late apoptotic and dead cell populations was identified as ultrasound PNP increased (Fig. 5a). For PNPs 0–185 kPa, there were 14% dead or dying cells, in comparison with 6% dead or dying in the controls. As a consequence of this observation, the 0–185 kPa PNPs condition was excluded in subsequent experiments.

Osteogenic gene expression post ultrasound treatment

On days 2 and 5, there were no significant differences between controls and cells exposed to 0–45 kPa PNP ultrasound in terms of *OSX* expression (Fig. 5b–g). However, there was 52% and 26% higher *OSX* expression in cells exposed to 0–108 kPa PNP ultrasound compared to control ($p < 0.05$) on day 2 and day 5, respectively. *RUNX2* expression levels were similar on day 2 for all conditions. On day 5 *RUNX2* expression increased with ultrasound PNP, with 17% and 26% higher expression for 0–45 and 0–108 kPa PNP ultrasound conditions, respectively compared to control ($p < 0.05$). A similar trend was observed for *bGLAP*, with 25% and 79% higher expression in 0–108 kPa PNP ultrasound condition compared to control on day 2 and day 5, respectively ($p < 0.05$), but it was 40% lower for 0–45 kPa PNP on day 5 compared to control ($p < 0.05$).

Assessment of ultrasound-exposed reseeded cells

After 1 day of reseeding, cells for all ultrasound exposure conditions (controls, 0–45 and 0–108 kPa PNP) showed similar cell morphologies

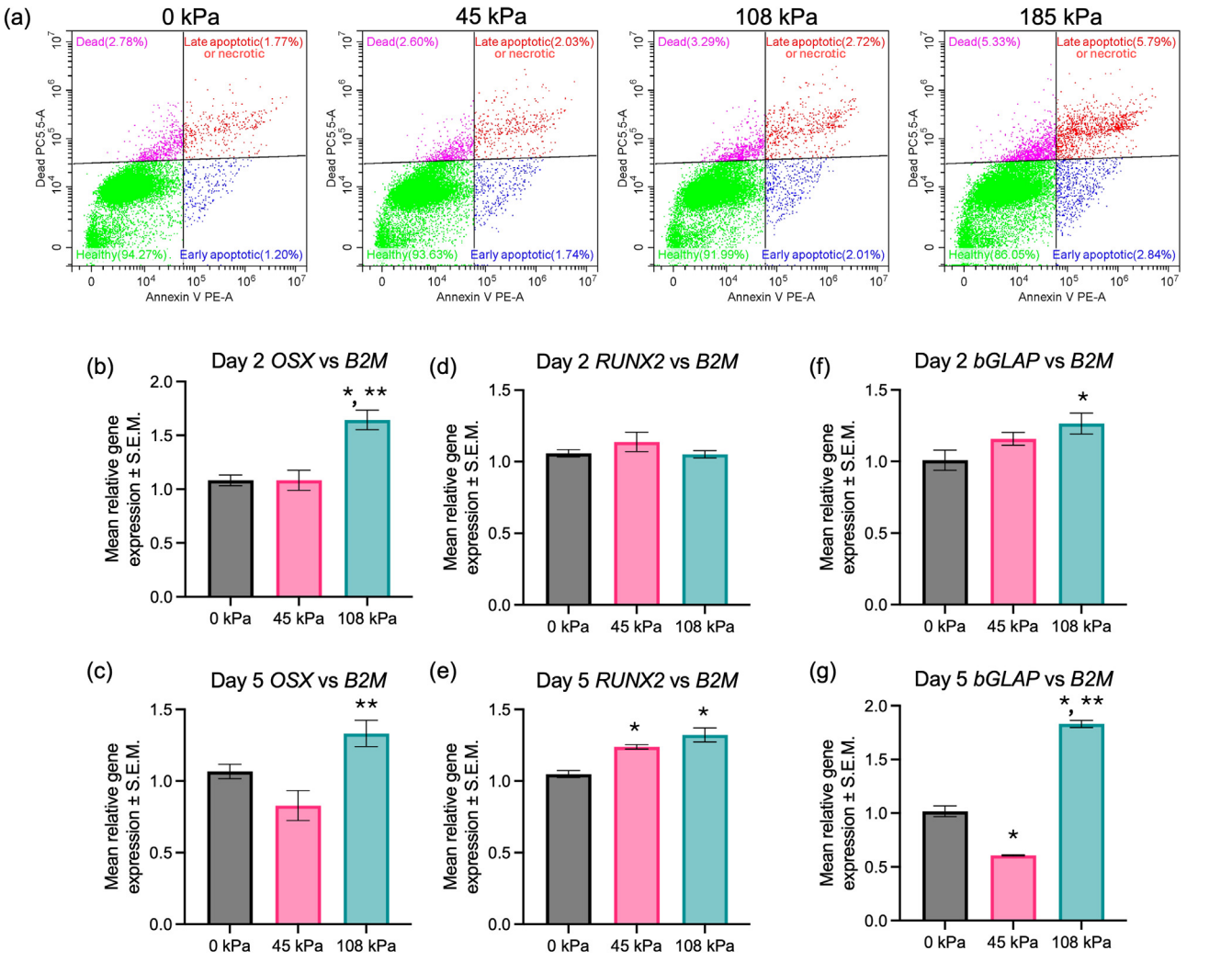

Figure 5. Effect of ultrasound on cells in cassette. (a) Apoptosis/necrosis assay for cells immediately after ultrasound exposure. There was a decrease in healthy cell population (*green*) and an increase in early apoptotic (*blue*), late apoptotic (*red*) as well as dead cell (*magenta*) populations as the ultrasound pressure increased at the centre of the cassette. Gene expression of cells after 2 (b, d, f) and 5 (c, e, g) days in culture. (b, c) *OSX*, (d, e) *RUNX2*, and (f, g) *bGLAP* (*osteocalcin*). Note the highest mean relative expression for all three genes on day 5 in the 108 kPa condition. * And ** indicate $p < 0.05$ relative to 0 and 45 kPa highest PNP conditions, respectively, $n = 3$. PNP, peak negative pressure.

with spindle shapes (Fig. 6a). There was also a similar number of cells present for all exposure conditions as assessed via DNA content measurements. When the culture period was extended to 7 and 15 days, there were again no significant differences between any of these conditions (Fig. 6b).

There was up to 60% and 25% downregulation of PINK1 (phosphatase and tensin homolog- induced kinase 1) and IP_3R (inositol 1,4,5-trisphosphate receptor) proteins expression respectively, in comparison to control for both ultrasound PNPs of 0–45 kPa ($p < 0.05$) and 0–108 kPa ($p \sim 0.06$) (Fig. 7a–d).

No significant differences in calcium deposition or collagen production were observed between the ultrasound PNPs for cells maintained in SC medium. In cells from OS medium there was 10% more calcium deposited as well as collagen produced for 0–45 kPa ultrasound PNPs, which was a statistically significant difference compared with other conditions ($p < 0.05$) (Fig. 8a–e).

Discussion

A standardised, quantifiable ultrasound dose delivery system is imperative when conducting *in vitro* investigations in the kHz ultrasound range. Correct measurement of the ultrasound dose delivered to the cells is essential to allow ultrasound effects to be linked to any biological changes detected.

The tank arrangement (Fig. 1) resulted in PNP hot spots at the centre of the measured ultrasound field at 5 and 25 mm distance from the transducer face, which aligned with the transducer long-axis. There were negligible reflections, from the water-absorber interfaces (at the tank walls) or at the water–air interface, evident in the scans at 5 mm distance from transducer face, with no other hot spots visible in the field data. However, at 25 mm distance the ultrasound field is asymmetrical and introduction of CLINIcell® cassette leads to the generation of a second hot spot; however, its measurement lies within the accuracy of the hydrophone and is much further away from where the cells were exposed to ultrasound. The CLINIcell® cassette placed in the path of the ultrasound had a transmission percentage of 80%, again within the error of hydrophone measurements (Fig. 3). Thus, it was concluded that the CLINIcell® cassette resulted in insignificant disruption to ultrasound wave propagation, meeting the requirement that it is acoustically transparent. This enabled precise measurement of ultrasound dose delivered to the cells in this study. Such a set-up enables reliable *in vitro*

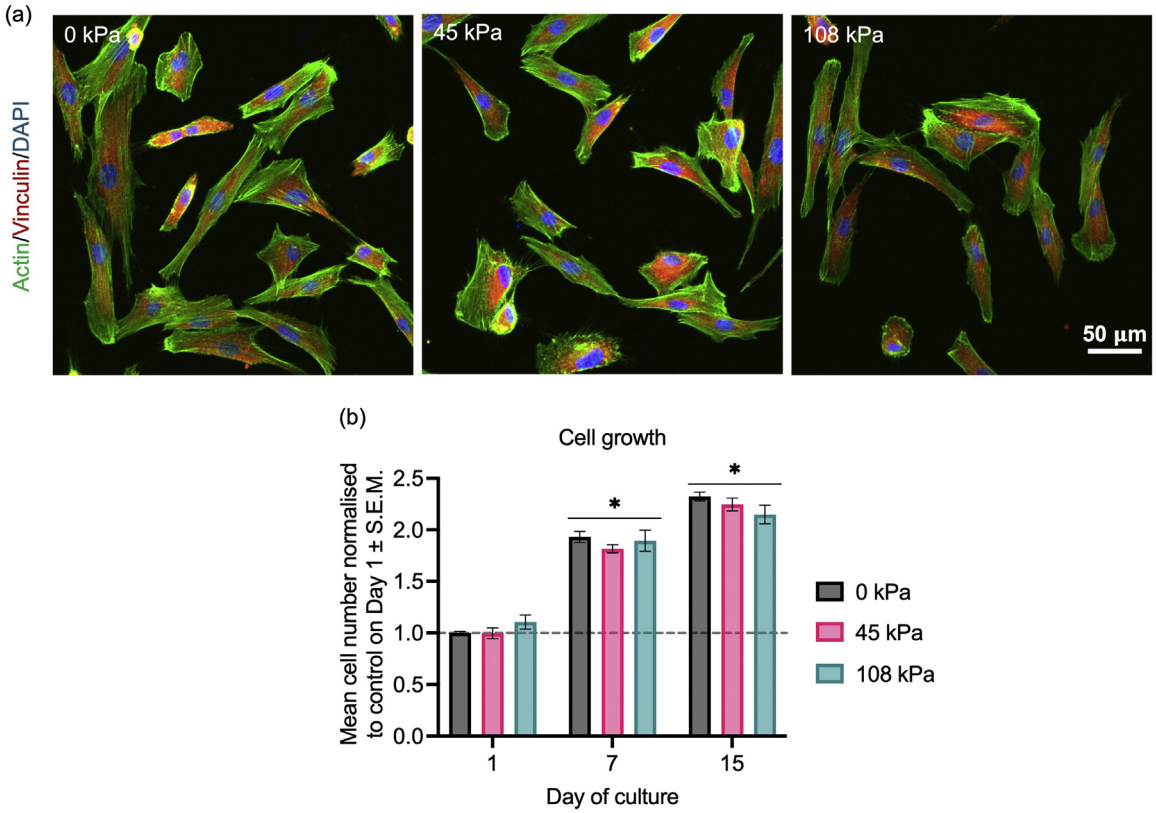

Figure 6. Assessment of morphology and growth of ultrasound-exposed reseeded cells. Representative images of actin (*green*), vinculin (*red*) and DAPI (*blue*) stained cells after 24 h of reseeding are shown. Their cells had similar morphology in all conditions. The mean cell numbers (measured via DNA content assay) all remained similar over 15 days of culture in all three conditions. * Indicates $p < 0.05$ compared with previous time points, $n = 3$. DAPI, 4′,6-diamidino-2-phenylindole.

assessments of biological effects in different cell types exposed to a range of low frequency ultrasound doses.

As the transducer driving current, and hence the vibration displacement of the anterior face of the transducer, increased (Fig. 2), cell death increased by 17% and the metabolic activity per cassette decreased by 27%, for the maximum PNP used in the study of 185 kPa. Moreover, cell detachment (42%) was mostly visible in the central region of the cassette where PNP was maximum. One-third of the dying cells were found to undergo stress-induced necrosis-like cell death whilst the remainder showed signs of apoptosis-like cell death [26] (Figs. 4 and 5a). This strongly suggested that higher PNP (>45 kPa) enhanced cell detachment and reduced cell survival. Moreover, not all the cells that detached from the cells were dying.

Other studies have also shown that osteogenic cell survival is affected by kHz ultrasound. A previous study showed that increasing the ultrasound intensity (from 10 to 75 mW/cm^2) led to increased osteogenic cell (Saos-2) death by inducing ER stress and membrane rupture in mitochondria [12]. These cells were seeded in traditional well plates or petri dishes and a Duo Son device was used to deliver continuous ultrasound (45 kHz, 5 min) to cells. In another study, Sura et al. [27] exposed rat primary osteoblasts (in a 35 mm petri dish) to 25 kHz continuous ultrasound for 30 s using a magnetostrictive ultrasound transducer and a TFI-1 tip (Dentsply, UK). There was increased cell death and decreased cell attachment as the transducer displacement increased. Scheven et al. [28] also showed a decrease in viability of odontoblast-like cells (on well plates) after exposure to a 30 kHz frequency D-tip scale probe for 3 min at intensities of 0.17 up to 0.92 W/cm^2. Hence, the relationship between osteogenic cell death and ultrasound pressure/intensity seems to be consistent and independent of the culture platform used, where higher PNP leads to cell death.

In this study, the cells exposed to ultrasound demonstrated upregulation of *OSX* and *RUNX2* expression, which sustained up to 5 days in culture, specifically for 0−108 kPa PNPs (Fig. 5b−g). This suggests that ultrasound can promote early osteogenic differentiation in hMSCs in the absence of osteogenic induction medium, easily detectable for 0−108 kPa PNPs range. When these cells were detached and reseeded on well plates, they had similar attachment efficiency and proliferation rate as the control cells during 2 weeks of normal culture (Fig. 6). More interestingly, the cells exposed to ultrasound lower than 45 kPa PNPs may have enhanced osteogenic potential for bone healing due to enhanced mineral and collagen production when cultured in osteogenic medium (Fig. 8).

Upregulation in osteogenesis has mostly been reported in the MHz frequency range, and within a few studies at 45 kHz frequency. Specifically, frequencies of 1−1.5 MHz have been shown to upregulate osteogenesis in MSCs via inhibition of PPAR-γ activation through ROCK-Cot/Tpl2-MEK-ERK pathway [29] and via activation of JNK, ERK1/2 and p38 MAPK pathways [30−32]. Hasegawa et al. [33] reported two and four times higher *OSX* and *RUNX2* expressions respectively, after 2 days of daily exposure to LIPUS (1.5 MHz, I_{SATA} 30 mW/cm^2, 20 min) in haematoma-derived progenitor cells from human tibia, fibula and clavicle. Lai et al. [34] also reported three times higher *RUNX2* expression after 1−4 weeks of daily exposure to LIPUS (1 MHz, I_{SATA} 200 mW/cm^2, 20 min). Some other studies also showed enhanced collagen production and calcium deposition in human mandibular osteoblasts when exposed to pulsed 1 MHz frequency ultrasound (100 mW/cm^2) or 45 kHz continuous frequency ultrasound (30 mW/cm^2) [35−37]. Direct comparison of these studies, between each other and with the present study, is difficult due to the variation in experimental set-ups and cells used as well as the unknown pressures experienced by cells in these studies due to the

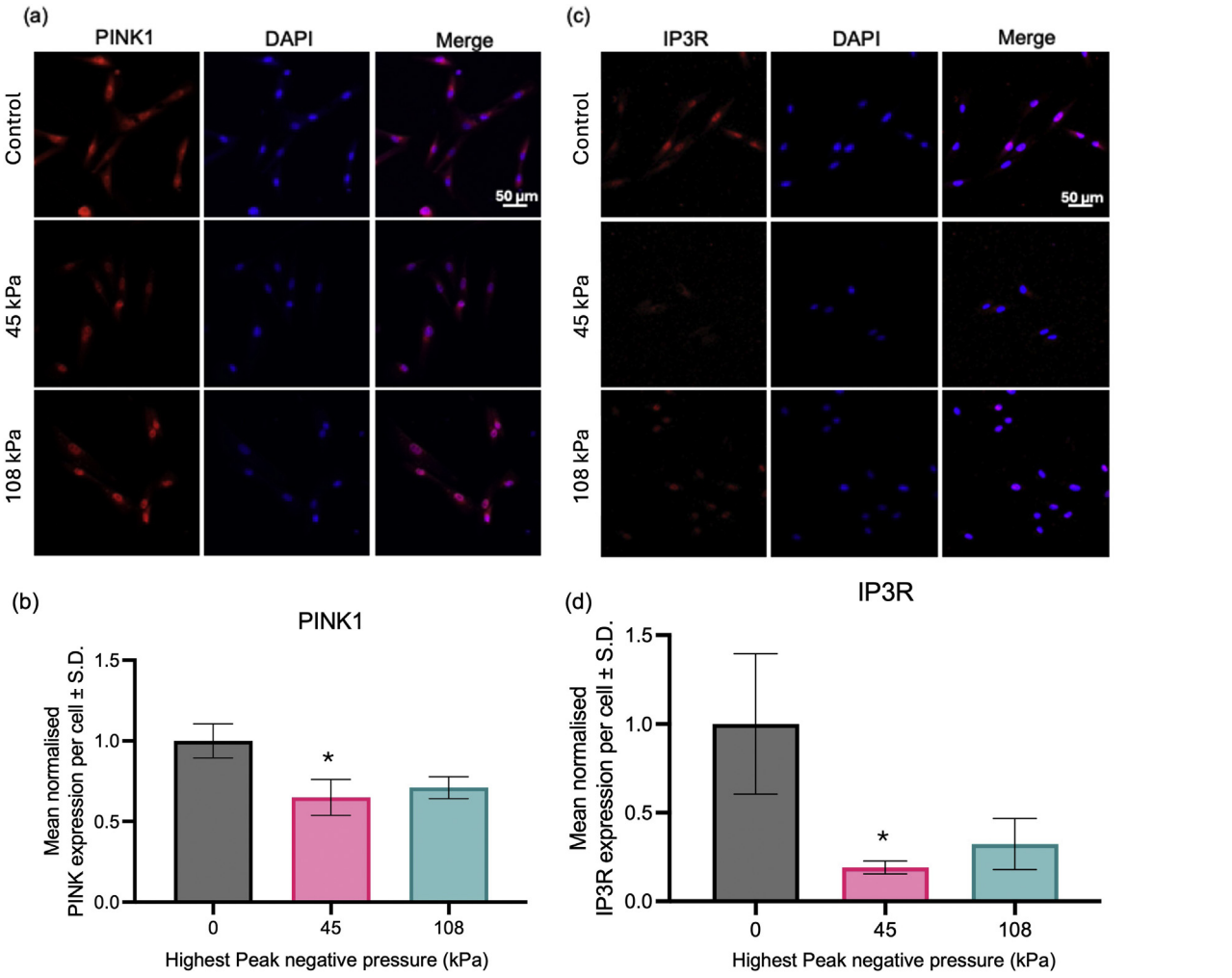

Figure 7. Assessment of PINK1 and IP_3R proteins expression by ultrasound exposed reseeded cells. Ultrasound exposure led to a drop in the expression of both proteins per cell. Representative images of PINK1 or IP_3R (*red*), DAPI (*blue*) with overlays after 24 h of reseeding are shown in (a) and (c). Signal quantification normalised to control (0 kPa) are shown in (b) and (d).* Indicates $p < 0.05$, $n = 10$ cells/condition. DAPI, 4′,6-diamidino-2-phenylindole.

use of non-standardised ultrasound delivery systems. Nonetheless, the present data confirmed that the therapeutic effect of ultrasound may not be limited to the MHz frequency range or 45 kHz frequency applied on a daily basis, but is also possible at a lower kHz frequency of 25 kHz with a single exposure of 5 min. However, it remains unclear if similar molecular mechanisms are involved and if longer exposure in continuous or pulsed mode could further enhance this effect, warranting further investigations.

Previous studies have also shown that mitochondrial stress can lead to release of Ca^{2+} into the cytosol [38] and an overload can induce apoptosis [39], which may be mitigated by downregulation of IP_3R (an intracellular calcium channel on the endoplasmic reticulum membrane) expression [40] as a protective mechanism. In relation to ultrasound treatment, it was found that a much higher frequency than used in the present study, of 47 MHz, can trigger the connexin 43 hemichannels on the plasma membrane of MSCs to open up and in effect release Ca^{2+} reserves from endoplasmic reticulum via the phospholipase C-inositol 1,4,5-trisphosphate (IP3) pathway [16]. In the present study, both PINK1 and IP_3R protein expression levels were reduced after ultrasound treatment (Fig. 7). This observation is in line with a previous study that showed mitochondrial damage and cell death in osteogenic cells (SaoS2) after 5 min of 45 kHz continuous ultrasound exposures at three different intensities of 10, 25 and 75 mW/cm^2 [12]. The current results also suggested that 25 kHz ultrasound may have dysregulated mitochondrial homeostasis via calcium release due to dysregulation of IP_3R. In the case of cells exposed to lower PNP, the Ca^{2+} release in cytosol may have been controlled by reduction in IP_3R expression (protective mechanism). On the other hand, at higher ultrasound PNP mitochondria may have been excessively damaged [12] causing failure to regulate IP_3R and, in some cells, instant death. It is also possible that the Ca^{2+} reserves released at <45 kPa PNPs condition may have been deposited into ECM, which was detectable on day 14 of osteogenic differentiation of hMSCs. Future work on calcium release and IP_3R and PINK1 expressions will explore this hypothesis.

Current findings suggest that careful control of ultrasound could minimise damage to hMSCs and potentially enhance bone regeneration. This has potential benefits for the use of ultrasonic bone surgery devices. If the ultrasonic surgical tip is within 5 mm of the bone marrow during surgery, a lower power setting, and hence lower ultrasonic displacement of the tip, may minimise MSC death and upregulate osteogenesis. This may be more relevant during surgeries of thinner bones in infants, children or in adults (e.g., jaw and fibula) where the bone marrow is more easily accessible and also for ultrasonic osteotomes, where it is important in surgery to minimise tissue damage, for example, in bone biopsies and bone grafting applications. Future *in vivo* bone-cutting experiments using

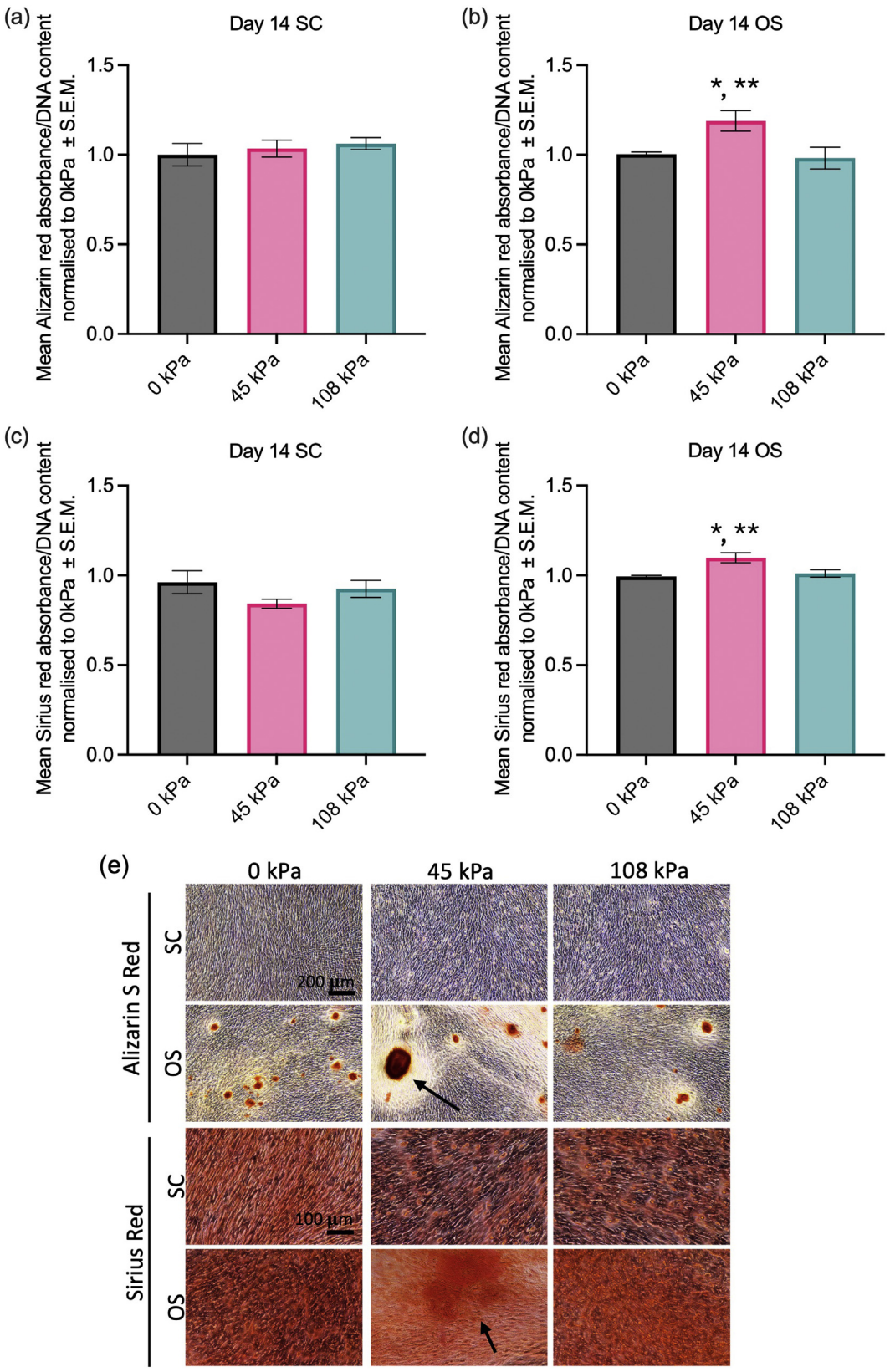

Figure 8. Assessment of mineralisation (a, b) and collagen (c, d) production by ultrasound exposed reseeded cells. There was highest mineral and highest collagen with visibly large nodules (e, *arrows*) at 45 kPa PNP in OS medium on day 14. * And ** indicate $p < 0.05$ relative to 0 and 108 kPa highest PNP conditions, respectively, $n = 3$. PNP, peak negative pressure.

surgical tools with 25 kHz ultrasound frequency will provide more reliable data to support this.

Conclusions

The tank-based ultrasound exposure system used in this study did not generate standing waves or reflections and ensured reliable delivery of quantifiable ultrasound doses. This methodology allows standardisation of kHz ultrasound delivery to assess cellular effects. MSCs survival and osteogenic differentiation were shown to be affected by the kHz continuous ultrasound with an application of 5 min duration. Specifically, lower ultrasound pressure (<45 kPa PNP at 25 kHz) had minimal impact on hMSC survival and enhanced osteogenic differentiation, and higher ultrasound pressure (>108 kPa PNP at 25 kHz) led to increased hMSC death through necrosis and apoptosis. A clear quantifiable ultrasound dose delivered to the MSCs will allow reliable clinical translation of observed biological effects for robust bone healing applications.

Data availability

The datasets generated during and/or analysed during the current study are available from the corresponding author upon request.

CRediT author statement

D.G. – Conceptualisation, Methodology, Validation, Formal analysis, Investigation, Data Curation, Writing-original draft, Visualisation, Project administration. X.L. – Conceptualisation, Methodology, Software, Formal analysis, Visualisation, Writing-Original Draft. J.S. – Writing-Review and Editing, Visualisation, Validation, Methodology, Formal analysis, Data curation. L.S. – Methodology, Validation, Data Curation, Writing – Review and Editing. H.M. – Software, Data Curation, Visualisation. P.M. – Validation, Writing – Review and Editing. R.M.S. – Methodology, Supervision, Funding acquisition, Writing – Review and Editing. B.A.S. – Supervision, Funding acquisition, Project administration, Writing – Review & Editing. M.L. – Supervision, Funding acquisition, Project administration, Writing – Review and Editing. A.D.W. – Supervision, Funding acquisition, Project administration, Writing – Review and Editing.

Conflict of interest

Author Lisa Shriane is employed by Elsevier. However, this employment began after the completion of research in this manuscript. The author had no involvement in the peer-review or editorial process of this article. The other authors declare no conflicts of interest.

Acknowledgements

This work is funded by the Engineering and Physical Sciences Research Council and part of the Ultrasurge Project under Grant EP/R045291/1. D.G. thanks Dr. Aleksander Marek and Dr. Robert Wallace for helpful discussions about ultrasound and standing waves. D.G. also thanks Mr. Ferdus Sheik, Flow Cytometry facility at University of Birmingham for assistance with flow cytometry.

Supplementary materials

Supplementary material associated with this article can be found, in the online version, at doi:10.1016/j.ultrasmedbio.2026.03.026.

References

[1] Pittenger MF, Mackay AM, Beck SC, Jaiswal RK, Douglas R, Mosca JD, et al. Multilineage potential of adult human mesenchymal stem cells. Science 1999;284:143–7.
[2] Higgins A, Glover M, Yang Y, Bayliss S, Meads C, Lord J. EXOGEN ultrasound bone healing system for long bone fractures with non-union or delayed healing: A NICE Medical Technology Guidance. Appl Health Econ Health Policy 2014;12:477–84.
[3] Mathieson A, Wallace R, Cleary R, Li L, Simpson H, Lucas M. Ultrasonic needles for bone biopsy. IEEE Trans Ultrason Ferroelectr Freq Control 2017;64:433–40.
[4] Wallace R, Spadaccino A, Leung A, Pan Z, Ganilova O, Muir A, et al. A comparison of past, present and future bone surgery tools. Int J Orthop 2015;2:266–9.
[5] Walmsley AD. Ultrasonic dental instrumentation. Power ultrasonics: applications of high-intensity ultrasound. 2nd ed. Elsevier; 2023.. p. 557–575..
[6] Bessen S, Gadkaree SK, Derakhshan A. Use of piezoelectric instrumentation in craniofacial surgery. Curr Opin Otolaryngol Head Neck Surg 2024;32:209–14.
[7] Zhang Y, Wang C, Zhou S, Jiang W, Liu ZH, Xu L. A comparison review on orthopedic surgery using piezosurgery and conventional tools. Procedia CIRP 2017;65:99–104.
[8] Labanca M, Azzola F, Vinci R, Rodella LF. Piezoelectric surgery: twenty years of use. Br J Oral Maxillofac Surg 2008;46:265–9.
[9] Anderson B, Mozaffari K, Foster CH, Jaco AA, Rosner MK. The ultrasonic bone scalpel does not outperform the high-speed drill: a single academic experience. World Neurosurg 2024;185:e387–96.
[10] Al-Namnam NM, Luczak AT, Yang I, Li X, Lucas M, Hall AC, Simpson H. Chondroprotection of articular cartilage integrity: Utilizing ultrasonic scalpel and hyperosmolar irrigation solution during cutting. Osteoarthr Cartil Open 2024;6:100499.
[11] Padilla F, Puts R, Vico L, Raum K. Stimulation of bone repair with ultrasound: a review of the possible mechanic effects. Ultrasonics 2014;54:1125–45.
[12] Gupta D, Savva J, Li X, Chandler JH, Shelton RM, Scheven BA, et al. Traditional multiwell plates and petri dishes limit the evaluation of the effects of ultrasound on cells *in vitro*. Ultrasound Med Biol 2022;48:1745–61.
[13] Patel US, Ghorayeb SR, Yamashita Y, Atanda F, Walmsley AD, Scheven BA. Ultrasound field characterization and bioeffects in multiwell culture plates. J Ther Ultrasound 2015;3:1–13.
[14] Snehota M, Vachutka J, GT Haar, Dolezal L, Kolarova H. Therapeutic ultrasound experiments *in vitro*: review of factors influencing outcomes and reproducibility. Ultrasonics 2020;107:106167.
[15] Riis Porsborg S, Krzyslak H, Pierchala MK, Trolé V, Astafiev K, Lou-Moeller R, et al. Exploring the potential of ultrasound therapy to reduce skin scars: an *in vitro* study using a multi-well device based on printable piezoelectric transducers. Bioengineering 2023;10:566.
[16] Feril LB, Kondo T, Zhao QL, Ogawa R, Tachibana K, Kudo N, et al. Enhancement of ultrasound-induced apoptosis and cell lysis by echo-contrast agents. Ultrasound Med Biol 2003;29:331–7.
[17] Savva J, Lucas M, Mulvana H. A controlled *in vitro* study of optimal low intensity pulsed ultrasound fields for stimulation of proliferation in murine osteoblasts. 2019 IEEE International Ultrasonics Symposium (IUS). IEEE; 2019. p. 1543–6.
[18] Beekers I, van Rooji T, van der Steen AFW, de Jong N, Verweij MD, Kooiman K. Acoustic characterization of the CLINIcell for ultrasound contrast agent studies. IEEE Trans Ultrason Ferroelectr Freq Control 2019;66:244–6.
[19] Beekers I, Langeveld SAG, Meijlink B, van der Steen AFW, de Jong N, Verweij MD, et al. Internalization of targeted microbubbles by endothelial cells and drug delivery by pores and tunnels. J Control Release 2022;347:460–75.
[20] Amps KJ, Jones M, Baker D, Moore HD. *In situ* cryopreservation of human embryonic stem cells in gas-permeable membrane culture cassettes for high post-thaw yield and good manufacturing practice. Cryobiology 2010;60:344–50.
[21] Roovers S, Lajoinie G, De Cock I, Brans T, Dewitte H, Braeckmans K, et al. Sonoprinting of nanoparticle-loaded microbubbles: unraveling the multi-timescale mechanism. Biomaterials 2019;217:119250.
[22] Gupta D, Grant DM, Hossain KMZ, Ahmed I, Sottile V. Role of geometrical cues in bone marrow-derived mesenchymal stem cell survival, growth and osteogenic differentiation. J Biomater Appl 2018;32:906–19.
[23] Yang YHK, Ogando CR, Wang See C, Chang TY, Barabino GA. Changes in phenotype and differentiation potential of human mesenchymal stem cells aging *in vitro*. Stem Cell Res Ther 2018;9:131.
[24] Velickovic K, Lugo Leija HA, Bloor I, Law J, Sacks H, Symonds M, et al. Low temperature exposure induces browning of bone marrow stem cell derived adipocytes *in vitro*. Sci Rep 2018;8:4974.
[25] Gupta D, Hossain KMZ, Roe M, Smith EF, Ahmed I, Sottile V, et al. Long-term culture of stem cells on phosphate-based glass microspheres: synergistic role of chemical formulation and 3D architecture. ACS Appl Bio Mater 2021;4:5987–6004.
[26] Gupta D, Martinez DC, Puertas-Mejía MA, Hearnden VL, Reilly GC. The effects of Fucoidan derived from *Sargassum filipendula* and *Fucus vesiculosus* on the survival and mineralisation of osteogenic progenitors. Int J Mol Sci 2024;25:2085.
[27] Sura H, Shelton RM, Walmsley AD. Osteoblast viability and detachment following exposure to ultrasound *in vitro*. J Mater Sci Mater Med 2001;12:997–1000.
[28] Scheven BA, Millard JL, Cooper PR, Lea SC, Walmsley AD, Smith AJ. Short-term in vitro effects of low frequency ultrasound on odontoblast-like cells. Ultrasound Med Biol 2007;33:1475–82.
[29] Kusuyama J, Bandow K, Shamoto M, Kakimoto K, Ohnishi T, Matsuguchi T. Low intensity pulsed ultrasound (LIPUS) influences the multilineage differentiation of mesenchymal stem and progenitor cell lines through ROCK-Cot/Tpl2-MEK-ERK signaling pathway. J Biol Chem 2014;289:10330–44.
[30] Gao Q, Walmsley AD, Cooper PR, Scheven BA. Ultrasound stimulation of different dental stem cell populations: role of mitogen-activated protein kinase signaling. J Endod 2016;42:425–31.
[31] Carina V, Costa V, Raimondi L, Pagini S, Sartori M, Figallo E, et al. Effect of low-intensity pulsed ultrasound on osteogenic human mesenchymal stem cells commitment in a new bone scaffold. J Appl Biomater Funct Mater 2017;15:e215–22.

[32] Sena K, Angle SR, Kanaji A, Aher C, Karwo DG, Sumner DR, et al. Low-intensity pulsed ultrasound (LIPUS) and cell-to-cell communication in bone marrow stromal cells. Ultrasonics 2011;51:639–44.
[33] Hasegawa T, Miwa M, Sakai Y, Niikura T, Kurosaka M, Komori T. Osteogenic activity of human fracture haematoma-derived progenitor cells is stimulated by low-intensity pulsed ultrasound *in vitro*. J Bone Joint Surg Br 2009;91:264–70.
[34] Lai CH, Chen SC, Chiu LH, Yang CB, Tsai YH, Zuo CS, et al. Effects of low-intensity pulsed ultrasound, dexamethasone/TGF-β1 and/or BMP-2 on the transcriptional expression of genes in human mesenchymal stem cells: Chondrogenic vs. osteogenic differentiation. Ultrasound Med Biol 2010;36:1022–33.
[35] Doan N, Reher P, Meghji S, Harris M. *In vitro* effects of therapeutic ultrasound on cell proliferation, protein synthesis, and cytokine production by human fibroblasts, osteoblasts, and monocytes. J Oral Maxillofac Surg 1999;57:409–19.
[36] Reher P, Doan N, Bradnock B, Meghji S, Harris M. Therapeutic ultrasound for osteoradionecrosis: an *in vitro* comparison between 1 MHz and 45 KHz machines. Eur J Cancer 1998;34:1962–8.
[37] Reher P, Harris M, Whiteman M, Hai HK, Meghji S. Ultrasound stimulates nitric oxide and prostaglandin E2 production by human osteoblasts. Bone 2002;31:236–41.
[38] Ren L, Chen X, Chen X, Li J, Cheng B, Xia J. Mitochondrial dynamics: fission and fusion in fate determination of mesenchymal stem cells. Front Cell Dev Biol 2020;8:580070.
[39] Decuypere JP, Monaco G, Bultynck G, Missiaen L, De Smedt H, Parys JB. The IP_3 receptor-mitochondria connection in apoptosis and autophagy. Biochim Biophys Acta Mol Cell Res 2011;1813:1003–13.
[40] Joseph SK, Hajnóczky G. IP_3 receptors in cell survival and apoptosis: Ca^{2+} release and beyond. Apoptosis 2007;12:951–68.